Macromolecular Rapid Communications
www.mrc-journal.de

Sn-Polyester/Polyimide Hybrid Flexible Free-Standing Film as a Tunable Dielectric Material

*Shamima Nasreen, Matthew L. Baczkowski, Gregory M. Treich, Mattewos Tefferi, Caroline Anastasia, Rampi Ramprasad, Yang Cao, and Gregory A. Sotzing**

Flexible films having high dielectric constants with low dielectric loss have promising application in the emerging area of high-energy-density materials. Here, for the first time, an organometallic, Sn-polyester-containing hybrid free-standing film in polyimide matrix is reported. Polyimide, pBTDA-HDA, is used with poly(dimethyltin glutarate) and poly(dimethyltin-3,3-dimethyglutarate) (pDMTDMG) for having a processable film with tunable dielectric properties. Hybrid film with 60% pDMTDMG and 40% PI (HB2) is found to have improved dielectric features over previously synthesized organic polyimide and organometallic Sn-polyester homopolymers. These novel organometallic–organic hybrid systems expanded a new area of dielectrics for next-generation electronics with superior overall electrical performance.

With the emerging technological advancement in the area of high-energy-density materials, the need for an effective dielectric medium for energy storage application with high dielectric constant (κ) and low dielectric loss (tan δ) has grown significantly over the recent years.[1] Dielectric materials, especially those exhibiting flexible and free-standing films are attractive for rapidly growing energy storage technology such as flex circuits, hybrid vehicles, wearable electronics, biomedical devices, power electronics, solar cells, and electrical weapon systems due to their ease of handling, space saving, light weight, and conformability. However, there are many challenges currently faced by the field of dielectric material synthesis and processing, which include the improvement of the κ while maintaining low tan δ in a thin film with a flexible free-standing ability. Generally, linear dielectrics with high κ, low tan δ and high breakdown strength will result in effective high energy densities. Traditional polymer dielectric films with high breakdown strength generally suffer from low κ, which limits their energy density.[2] The current industry standard, biaxially oriented polypropylene (BOPP) film is useful for its ultra-low tan δ (<0.001) and high band gap (E_g). However, low κ (≈2.1) and low operation temperature (85 °C) of BOPP limits its practical use in many high energy density and high temperature applications. Recently, a rational co-design process of discovering new dielectric materials based on iterative ab initio computation suggests that the electronic polarization for non-polar materials like BOPP correlates inversely with the band gap and thus cannot be enhanced without affecting the latter.[3,4] On the contrary, such correlations are not observed for ionic polarizations found in organometallic polymers.[5]

Organometallic polymers containing metal atoms in the backbone such as tin complexation systems were studied by our team with the aid of the rational co-design process.[6,7] These newly developed organometallic Sn-polyesters systems exhibit high κ (>6) and have excellent agreement with the computational predictions in terms of structure and electrical properties like κ and E_g.[6–9] Among the various Sn-polyester systems, the poly(dimethyltin glutarate) (pDMTGlu)[6] and poly(dimethyltin-3,3-dimethyl glutarate) (pDMTDMG)[7] have higher $\kappa \approx 6.1$ and ≈6.3, respectively, with low loss compared to all Sn-polyesters studied. pDMTGlu has three methylene spacers in their repeat unit, whereas, pDMTDMG has two additional methyl groups attached to the C-3 position shown in **Figure 1**D. However, pDMTGlu forms fractal crystal patterns upon drying, which results in a brittle film on a metal substrate with low breakdown strength. On the other hand, the branched methyl groups in pDMTDMG play a significant role in preventing aggregation in the polymer matrix when blended with a second Sn-polyester system by disrupting the chain packing.[6]

Recently, polyimides (PIs) containing hybrid materials are of great interest and are receiving extensive consideration due to their improved morphological, thermal, and electrical properties.[1,10–13] PI with a dianhydride, 3,3′,4,4′-benzophenonetetracarboxylic dianhydride (BTDA), and an aliphatic diamine linker 1,6-hexadiamine (HDA) was also synthesized by our team.[3,14] The rigidity of the aromatic repeat unit gives strength and stability to the polymer, leading to high T_g, whereas the flexible

S. Nasreen, C. Anastasia, Prof. G. A. Sotzing
Department of Chemistry
University of Connecticut
55 N Eagleville Road, Storrs, CT 06269, USA
E-mail: g.sotzing@uconn.edu
M. L. Baczkowski, G. M. Treich
Institute of Materials Science
University of Connecticut
97 N Eagleville Road, Storrs, CT 06269, USA
M. Tefferi, Prof. Y. Cao
Electrical Insulation Research Center
University of Connecticut
Storrs, CT 06269, USA
Prof. R. Ramprasad
School of Materials Science and Engineering
Georgia Institute of Technology
Atlanta, GA 30332, USA
The ORCID identification number(s) for the author(s) of this article can be found under https://doi.org/10.1002/marc.201800679.

DOI: 10.1002/marc.201800679

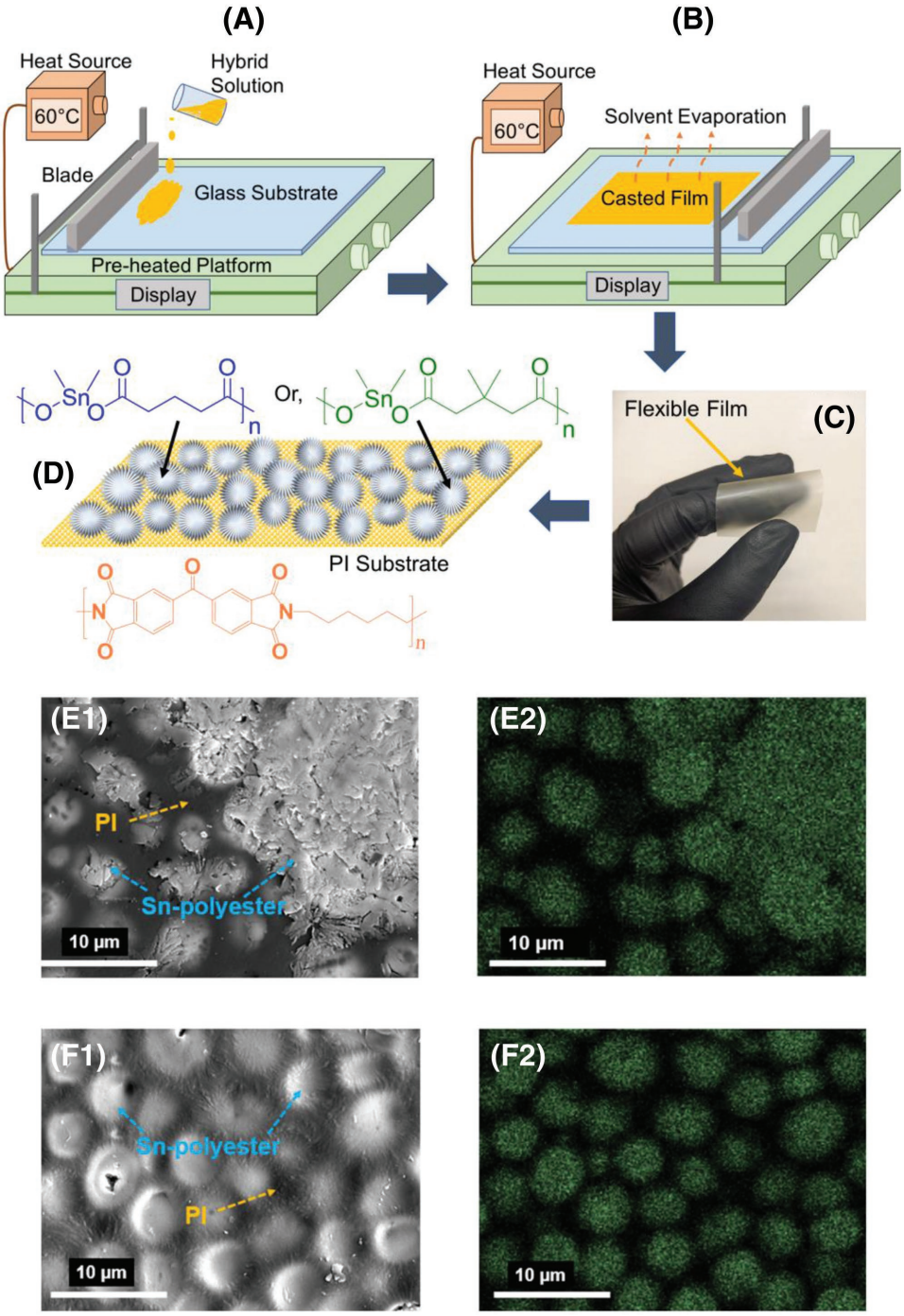

Figure 1. Cartoon representation of Sn-polyester/PI hybrid film processing A) before solution casting, B) after casting on Doctor Blade coater; C) HB2 film after solvent evaporation and vacuum drying, and D) cartoon morphology of the dried film showing the distribution of Sn-polyester in PI. FE-SEM morphology of E1) HB1 (p(DMTGlu60%-BTDAHDA40%)) and F1) HB2 (p(DMTDMG60%-BTDAHDA40%)) showing the distribution of Sn-polyester in PI substrates, E2,F2) for the elemental mapping of Sn (green dots) in HB1 and HB2, respectively.

aliphatic spacer improves the morphology and mobility of the chain.[14] However, the pBTDA-HDA exhibits relatively low $\kappa \approx 3.5$ with tan δ of 1% at 1 kHz.[14]

Herein, we produced hybrid films of Sn-polyester/PI using a polymer blend technique. The goal of this study was to produce a flexible, free-standing film of organometallic–organic hybrid out of our best-known Sn-polyester and polyimide systems with tunable dielectric properties, and in line with this to find an optimal condition to achieve the maximum κ while maintaining low tan δ without sacrificing the high band gap and breakdown strength for maximum potential energy density. In this work, a comparative study was reported for the pDMTDMG/

Table 1. Experimental dielectric constant (κ) and dissipation factor (tan δ) at 1 kHz, band gap energy (E_g), DC breakdown field from Weibull distribution analysis, breakdown field from *D–E* hysteresis loop, energy density at its highest field from DC breakdown strength and (from *D–E* loop are shown in parenthesis) for HB1 and HB2 films and previously synthesized polymers along with BOPP at room temperature are tabulated.

Polymer	κ at 1 kHz	tan δ at 1 kHz	E_g (eV)	DC breakdown [MV m^{-1}]	Breakdown from *D–E* loop [MV m^{-1}]	Energy density [J cm^{-3}]
BOPP	2.2[a)]	0.005[a)]	7.0[a)]	730[a)]	630[b)]	5.0[a)]
HB1	5.9	0.058	3.5	335	286	3.0 (2.5)
HB2	6.3	0.041	5.3	464	352	6.0 (5.6)
pDMTGlu[8]	6.1	0.015	4.7	N/A	N/A	N/A
pDMTDMG[9]	6.4	0.013	4.8	N/A	N/A	N/A
pBTDA-HDA[13]	3.4	0.005	3.4	812	N/A	9.8

[a)]Data from ref. [28]; [b)]Data from refs. [29,30].

pBTDA-HDA and pDMTGlu/pBTDA-HDA hybrids, showing their improved electrical performance over one another and from previously synthesized homopolymers

The optimal condition for making processable films was obtained by varying the blend ratios of the Sn- polyester. The maximum concentration of Sn-polyester was 60% w/w blended with 40% w/w of PI for having smooth free-standing film. The 60% pDMTGlu and 60% pDMTDMG hybrids are named as HB1 and HB2, respectively. Above this threshold the film became brittle due to its increased portion of the crystalline Sn-polyester moiety. Figure 1 shows the processing of a film along with the microfeatures. Here, in **F1** the PI acts as a matrix and pDMTDMG dispersed into it. The amorphous nature of the pDMTDMG helped the system to be more evenly distributed in the PI substrate with small phase separation compared to the pDMTGlu. For HB1, large microphase separation occurred due to the crystalline nature of pDMTGlu, resulting in large coagulation evident in **E2**. It is also evident from the elemental mapping in **F2** that the tin–oxygen ratio (green dots) has uniform distribution of the spherulite, whereas, in **E1** large clusters forms.

Films also exhibited weak dipole–dipole interaction between the polar polymers due to the presence of electron-rich imide bonds and electropositive Sn atom from Sn–O linkages evident in normalized FTIR spectra in Figure S1, Supporting Information for HB1 and HB2. The reduction of imide stretching at 1704 cm^{-1} occurred in both systems. The asymmetric stretching of CO bond at 1567 cm^{-1} in pDMTGlu and at 1614 cm^{-1} for pDMTDMG, was also reduced in HB1 and HB2, respectively, due to the weak interaction between the chains. The thermal stability was examined by TGA isothermally under a nitrogen atmosphere (Figure S2, Supporting Information) for HB1 and HB2. The glass transition temperature (T_g) of the HB2 (≈141 °C) was also higher than HB1 (≈119 °C) (Figure S3, Supporting Information). HB2 was annealed at elevated temperature to check if there were any morphological changes that had taken place. No changes had been observed in HB2 which was evident by the WAXD pattern shown in Figure S4, Supporting Information indicating the morphological stability of the film up to 200 °C. It can be argued that HB2 can be useful for high temperature (>100 °C) thin film dielectric applications.

Frequency-dependent dielectric behavior at room temperature is shown for all compositions in **Figure 2**A,B. By increasing the Sn-polyester concentration from 10% to 60%, κ also increases. Loss also increases by the incorporation of the Sn-polyesters, mostly in the higher frequency regions. Lower loss is observed for the pDMTDMG hybrids (0.007–0.041) compared to pDMTGlu hybrids (0.009–0.058), which is much lower than any known hybrid system.[1,11,12,15–22] Their trends in the κ and tan δ at 1 kHz in room temperature are shown in Figure 2C,D for all compositions. κ lies between the edges of two homopolymers such as from 3.5 to 6.1 for pDMTGlu and from 3.5 to 6.4 for pDMTDMG hybrids with PI. They showed very little frequency dependency on κ, which is indicative of a fast polarization response. The highest κ was observed for HB1 and HB2 systems with 5.9 and 6.3 at 1 kHz with a tan δ of ≈0.058 and ≈0.041, respectively, acceptable for many practical applications.

Dielectric response comprises different polarization mechanisms such as electronic, ionic, dipolar (orientational), and interfacial.[23] At very low temperatures, the orientational polarization is less prominent due to insufficient energy to overcome the rotation barriers. With the increase of temperature, dipolar polarization increases and can contribute to the overall polarization response and hence increase the κ. Here, the improvement of κ with the incorporation of the polar Sn-polyester is attributed to the enhanced ionic polarization, which is caused due to the presence of the highly polarizable Sn–O bond. At lower frequencies (i.e., <10 kHz), an upturn in tan δ was observed. Upon increasing the temperature, these peaks shifted to higher frequencies, which can be an indication of interfacial polarization, a typical characteristic of hybrids.[24,25] Studies show that interfacial polarization can contribute to the loss peak, especially at low frequency regions where temperature is a controlling factor.[11,24,25] Generally, with an increase in temperature, loss factor also increases due to the increased bulk conduction loss.[11,15,25,26] At 150 °C κ remains above 4.6 for HB1 and 5.1 for HB2 (Figure S5, Supporting Information) at 1 kHz. tan δ remained below 0.06 for HB2 and 0.10 for HB1 at 150 °C. However, overall dielectric loss for the HB2 (<≈0.02) was lower compared to HB1 (<≈0.04). The branched methyl groups hinder the chain packing and create more room to relax the chain. In contrast to that for hybrid system, interfaces also play a role in controlling the conduction loss via the trap formation for reduced electronic conductivity.[25,27]

For an insulating material, their dielectric breakdown mainly depends on intrinsic (composition of the system, underlying chemistry of the materials, bonding, etc.) as well as extrinsic factors.[31] The basic mechanism of polymer breakdown can be understandable by electron avalanche theory. Polymer breakdown occurs when high enough electric field promotes electrons from valence band to the conduction band to an extent that it creates electron avalanche.[14] Thus, for a defect free and pure dielectric material, band gap energy (E_g) can be an

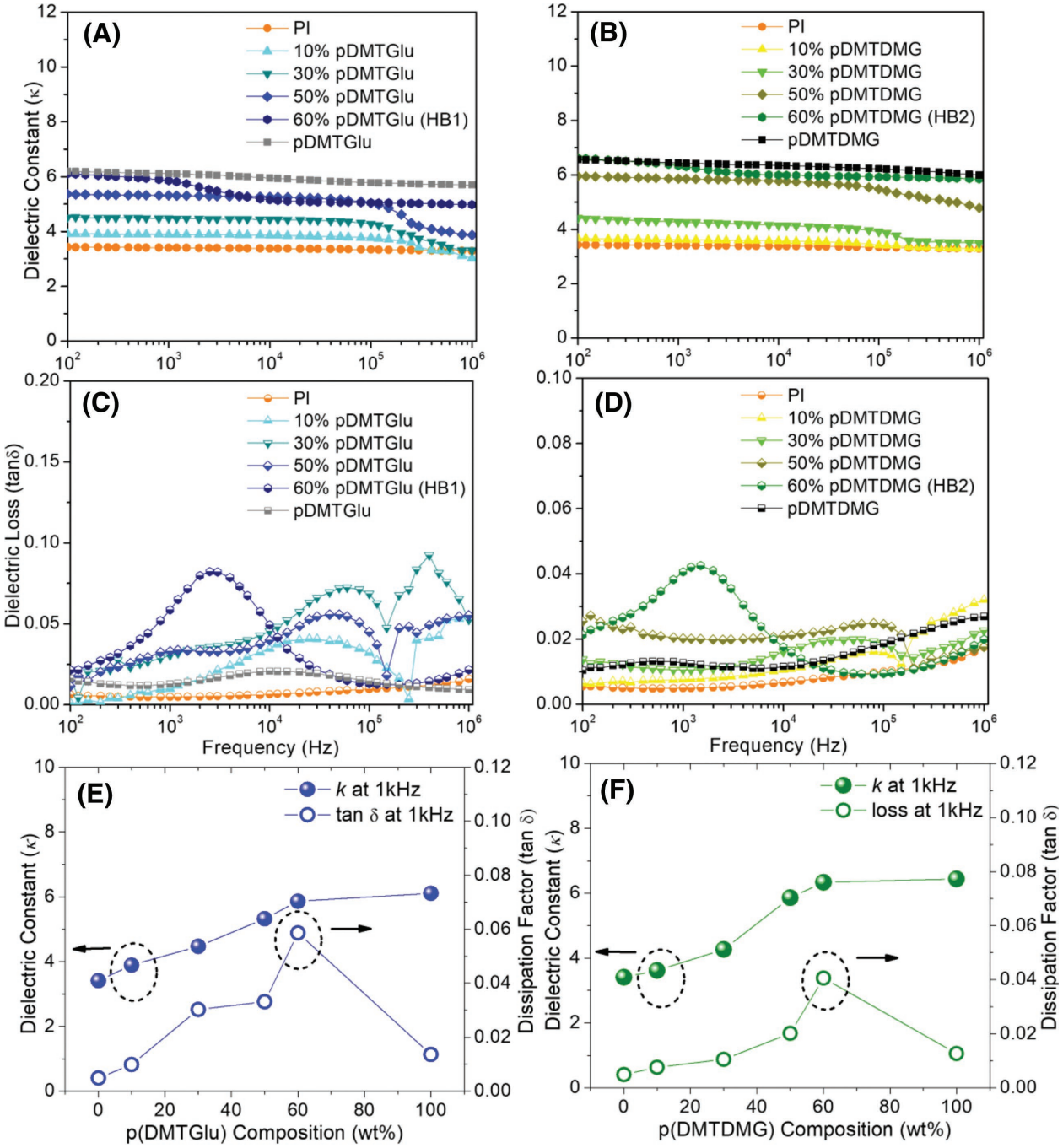

Figure 2. Frequency-dependent dielectric constant (κ) and dissipation factor (tan δ) of A,C) pDMTGlu/PI and B,D) pDMTDMG/PI hybrids, respectively, along with homopolymers PI, pDMTGlu, and pDMTDMG in the frequency range 100–1 MHz at room temperature. E,F) Dielectric constant (κ) and dissipation factor (tan δ) versus Sn-polyester composition in PI at 1 kHz of pDMTGlu and pDMTDMG systems, respectively.

approximation for the intrinsic breakdown.[9,31,32] This can be measured through the onset wavelengths of absorption from the UV–vis spectrum.[31–36] For a dielectric material, $E_g > 3$ eV is generally considered as useful for dielectric application. Here, E_g was found to be 3.25 and 5.32 eV for HB1 and HB2, respectively. The branched Sn-polyester in HB2 having more free volume compared to the linear Sn-polyester in HB1, which hindered the dipole–dipole interaction and reduced the charge carrier mobility, resulted in a wider band gap for HB2. However, establishing the relationship between the intrinsic breakdown and band gap is challenging due to the macroscopic imperfections (amorphous or semi-crystalline nature of the polymer matrix) as well as other factors like thermal, partial charge, and free volume breakdown.[14]

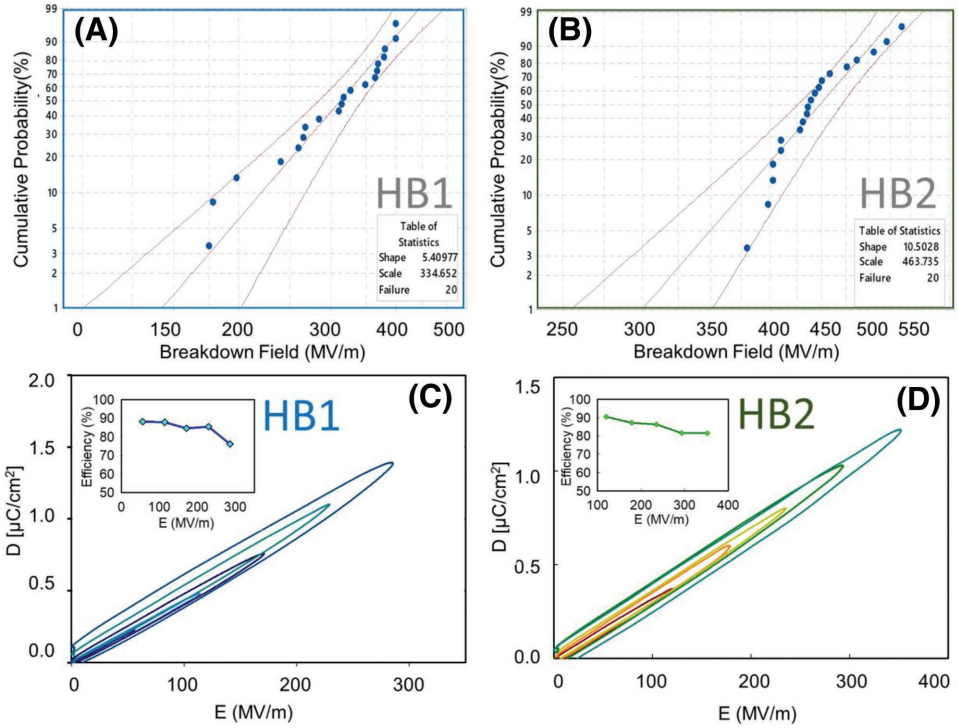

Figure 3. A,B) Weibull breakdown statistic plots for HB1 and HB2 films, respectively, showing breakdown strengths of 334 and 463 kV mm^{-1}, respectively. Charge–discharge (*D*–*E*) hysteresis loop of C) HB1 and D) HB2 films showing the breakdown voltage; inset is the corresponding efficiency with respect to applied voltage.

For HB1, the engineering DC breakdown strength at which 63.2% of the samples had broken down was 335 MV m^{-1} and that for HB2 was 464 MV m^{-1}. Hence, the potential energy density calculated at nearly DC breakdown field could be as high as 2.9 J cm^{-3} for HB1 and 5.9 J cm^{-3} for HB2 tabulated in Table 1. Experimental breakdown strengths are currently lower than PI due to processing conditions contributing a gap between intrinsic and actual performance. The presence of interface, microphase segregation of the Sn-polyesters within the polyimide, and higher free volume might result in localized field enhancement and could initiate early breakdown. Based on the calculated band gap, if these challenges could be overcome, the potential for improved performance could be high. The charge–discharge behavior was estimated by *D*–*E* hysteresis loop shown in **Figure 3**C and Figure 3D for HB1 and HB2, respectively. Breakdown fields found from the D–E hysteresis loop were 286 and 352 MVm^{-1} for HB1 and HB2, respectively; slightly lower than DC breakdown field. Hysteresis observed in the loop might have originated from the conduction loss at high voltage, which can be attributed to the interfacial relaxation and presence of impurities. The efficiency at the highest field, for the HB1 and HB2 was approximately 76% and 82%, respectively.

We have developed hybrid flexible free-standing semi-transparent films of organometallic Sn-polyester blended with polyimide pBTDA-HDA having tunable κ upon the addition of Sn-polyester. The maximum achievable κ for both pDMTGlu/PI and pDMTDMG/PI films having 60% load of tin-polyester ranges from ≈5.5 to 6.2, close to that of the tin homopolymers. These values show clear improvement over polyimide pBTDA-HDA having a κ of ≈3.5 while maintaining low dielectric loss with minimum frequency dispersion over a wide temperature range. The blend of 60% pDMTDMG with 40% polyimide stands out by their morphological and electrical properties showing a breakdown strength of 464 MV m^{-1}, with a maximum energy density of ≈6.0 J cm^{-3}. Band gap energy (5.3 eV) of this hybrid is higher than polyimide and tin homopolymers, which suggests an improved intrinsic breakdown strength. We have overcome the barrier of having ferroelectric behavior observed in the typical metal containing dielectric systems. This study opens a door to the other organometallic hybrid systems to consider as prospective dielectric candidate.

Supporting Information

Supporting Information is available from the Wiley Online Library or from the author.

Acknowledgements

This work was supported through the Office of Naval Research grant (N00014-16-1-2580). The authors would like to acknowledge JoAnne Ronzello for assisting in electrical measurements.

Conflict of Interest

The authors declare no conflict of interest.

Keywords

dielectrics, free-standing films, hybrids, polyimides, Sn-polyesters

Received: September 11, 2018
Revised: October 28, 2018
Published online:

[1] Z. M. Dang, T. Zhou, S. H. Yao, J. K. Yuan, J. W. Zha, H. T. Song, J. Y. Li, Q. Chen, W. T. Yang, J. Bai, *Adv. Mater.* **2009**, *21*, 2077.
[2] Z. Li, G. M. Treich, S. K. Scheirey, G. A. Sotzing, Y. Cao, presented at 2017 IEEE Conf. on Electrical Insulation and Dielectric Phenomena, Fort Worth, TX, October **2017**, p. 78.
[3] A. Mannodi-Kanakkithodi, G. M. Treich, T. D. Huan, R. Ma, M. Tefferi, Y. Cao, G. A. Sotzing, R. Ramprasad, *Adv. Mater. 28*, **2016**, 6277.
[4] A. Mannodi-Kanakkithodi, T. D. Huan, R. Ramprasad, *Chem. Mater.* **2017**, *29*, 9001.
[5] A. Mannodi-Kanakkithodi, A. Chandrasekaran, C. Kim, T. D. Huan, G. Pilania, V. Botu, R. Ramprasad, *Mater. Today* **2017**, *21*, 785.
[6] A. F. Baldwin, R. Ma, A. Mannodi-Kanakkithodi, T. D. Huan, C. Wang, M. Tefferi, J. E. Marszalek, M. Cakmak, Y. Cao, R. Ramprasad, G. A. Sotzing, *Adv. Mater.* **2015**, *27*, 346.
[7] G. M. Treich, S. Nasreen, A. Mannodi-Kanakkithodi, R. Ma, M. Tefferi, J. Flynn, Y. Cao, R. Ramprasad, G. A. Sotzing, *ACS Appl. Mater. Interfaces* **2016**, *8*, 21270.
[8] A. F. Baldwin, T. D. Huan, R. Ma, A. Mannodi-Kanakkithodi, M. Tefferi, N. Katz, Y. Cao, R. Ramprasad, G. A. Sotzing, *Macromolecules* **2015**, *48*, 2422.
[9] A. F. Baldwin, R. Ma, T. D. Huan, Y. Cao, R. Ramprasad, G. A. Sotzing, *Macromol. Rapid Commun.* **2014**, *35*, 2082.
[10] X. Chen, K. E. Gonsalves, G. -M Chow, T. D. Xiao, *Adv. Mater.* **1994**, *6*, 481.
[11] Q. Chi, J. Sun, C. Zhang, G. Liu, J. Lin, Y. Wang, X. Wang, Q. Lei, *J. Mater. Chem. C* **2014**, *2*, 172.
[12] Y. Wang, Q. Ge, X. Chen, S. Qi, G. Tian, D. Wu, *Macromol. Mater. Eng.* **2017**, *302*, 1.
[13] Y. Yang, B. Zhu, Z. Lu, Z. Wang, C. Fei, D. Yin, R. Xiong, J. Shi, Q. Chi, *APL Mater.* **2013**, *102*, 042904.
[14] R. Ma, A. F. Baldwin, C. Wang, I. Offenbach, M. Cakmak, R. Ramprasad, G. A. Sotzing, *ACS Appl. Mater. Interfaces* **2014**, *6*, 10445.
[15] Z. Zhu, Y. Yang, J. I. E. Yin, X. Wang, Y. Ke, Z. Qi, *J. Appl. Polym. Sci.* **1999**, *73*, 2063.
[16] Q. Chi, Z. Gao, C. Zhang, Y. Cui, J. Dong, X. Wang, Q. Lei, *J. Mater. Sci.: Mater. Electron.* **2017**, *28*, 15142.
[17] Q. G. Chi, J. F. Dong, C. H. Zhang, C. P. Wong, X. Wang, Q. Q. Lei, *J. Mater. Chem. C* **2016**, *4*, 8179.
[18] J. Chen, X. Wang, X. Yu, L. Yao, Z. Duan, Y. Fan, Y. Jiang, Y. Zhou, Z. Pan, *J. Mater. Chem. C* **2018**, *6*, 271.
[19] S. Han, J. Zhang, B. Teng, C. Ji, W. Zhang, Z. Sun, J. Luo, *J. Mater. Chem. C* **2017**, *5*, 8509.
[20] Y. Yang, H. Sun, D. Yin, Z. Lu, J. Wei, R. Xiong, J. Shi, Z. Wang, Z. Liu, Q. Lei, *J. Mater. Chem. A* **2015**, *3*, 4916.
[21] J. Wu, S. Yang, S. Gao, A. Hu, J. Liu, L. Fan, *Eur. Polym. J.* **2005**, *41*, 73.
[22] X. Fang, X. Liu, Z.-K. Cui, J. Qian, J. Pan, X. Li, Q. Zhuang, *J. Mater. Chem. A* **2015**, *3*, 10005.
[23] T. D. Huan, S. Boggs, G. Teyssedre, C. Laurent, M. Cakmak, S. Kumar, R. Ramprasad, *Prog. Mater. Sci.* **2016**, *83*, 236.
[24] Y. Feng, W. L. Li, Y. F. Hou, Y. Yu, W. P. Cao, T. D. Zhang, W. D. Fei, *J. Mater. Chem. C* **2015**, *3*, 1250.
[25] X. Chen, J.-K. Tseng, I. Treufeld, M. Mackey, D. Schuele, R. Li, M. Fukuto, E. Baer, L. Zhu, *J. Mater. Chem. C* **2017**, *5*, 10417.
[26] X. Liu, J. Yin, M. Chen, W. Bu, W. Cheng, Z. Wu, *Nanosci. Nanotechnol. Lett.* **2011**, *3*, 226.
[27] X. Liao, Y. Ding, L. Chen, W. Ye, J. Zhu, H. Fang, H. Hou, *Chem. Commun.* **2015**, *51*, 10127.
[28] G. M. Treich, M. Tefferi, S. Nasreen, A. Mannodi-Kanakkithodi, Z. Li, R. Ramprasad, G. A. Sotzing, Y. Cao, *IEEE Trans. Dielectr. Electr. Insul.* **2017**, *24*, 732.
[29] S. Nasreen, G. M. Treich, M. L. Baczkowski, A. K. Mannodi-Kanakkithodi, Y. Cao, R. Ramprasad, G. Sotzing, *Kirk-Othmer Encycl. Chem. Technol.* **2017**, 1, https://onlinelibrary.wiley.com/doi/abs/10.1002/0471238961.koe00036.
[30] S. Wu, W. Li, M. Lin, Q. Burlingame, Q. Chen, A. Payzant, K. Xiao, Q. M. Zhang, *Adv. Mater.* **2013**, *25*, 1734.
[31] L. M. Wang, presented at 25th Int. Conf. on Microelectronics, Belgrade, Serbia, May **2006**, p. 615, https://ieeexplore.ieee.org/abstract/document/1651032.
[32] Y. Ohki, N. Fuse, T. Arai, presented at 2010 Annual Report Conf. on Electrical Insulation and Dielectric Phenomena, West Lafayette, IN, October **2010**, https://ieeexplore.ieee.org/abstract/document/5723991.
[33] D. Grojo, M. Gertsvolf, H. Jean-Ruel, S. Lei, L. Ramunno, D. M. Rayner, P. B. Corkum, *Appl. Phys. Lett.* 243118, **2008**, *93*.
[34] W. J. Yin, X. G. Gong, S. H. Wei, *Phys. Rev. B* **2008**, *78*, 161203(R).
[35] P. P. González-Borrero, F. Sato, A. N. Medina, M. L. Baesso, A. C. Bento, G. Baldissera, C. Persson, G. A. Niklasson, C. G. Granqvist, A. Ferreira Da Silva, *Appl. Phys. Lett.* **2010**, *96*, 061909.
[36] N. Ghobadi, *Int. Nano Lett.* **2013**, *3*, 2.

